A Seismic Analysis of SP Graben in the San Francisco Volcano Field, AZ

University of Maryland - Department of Geology
Austin Hoyle
Advisors: Dr. Nicholas Schmerr - Dr. Vedran Lekic
GEOL394

Introduction

The volcanic structures within the San Francisco Volcano Field (SFVF) appear to have formed with preferential alignment, specifically those near SP Crater. Buried by an ancient lava flow near SP Crater, a portion of the Mesa Butte Fault System is visible at the surface in the north (Fig. 1). This project sought to use a seismic reflection analysis to detect the presense of Fault A and B, which together make SP Graben, in the subsurface beneath Volcanic Vent 5704. This presence could indicate the lava that formed the volcanic structures in the area used these faults as a pathway to reach the surface.

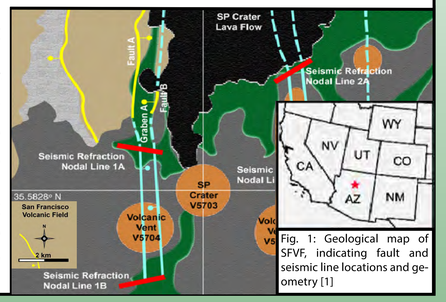

Fig. 1: Geological map of SFVF, indicating fault and seismic line locations and geometry [1]

Analog Motivation

Volcanic activity is one of the few geological processes that is uniformly expected to occur on the surface of all terrestrial planets. Investigating terrestrial analog environments like the SFVF informs reseachers about past and present geological processes occuring on other planets. This project's objective is similar to what may be of interest in the future on the moon or Mars and improving upon geophysical processes here on earth can inform future investigations elsewhere in our solar system.

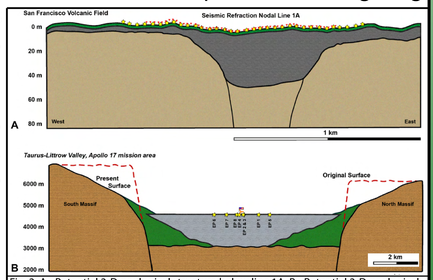

Fig. 2: A - Potential 2-D geological structure below line 1A. B - Potential 2-D geological structure at Taurus-Littrow Valley, the Apollo 17 mission area [1].

Hypothesis

SP Graben has southward continuation beyond Volcanic Vent 5704.

Data

Data used for this project were aquired by Bell (2021). Raw seismic data were converted to SEG-Y format. Data were measurements of ground displacement following a seismic disturbance, or a shot, recorded at 2000 Hz, and were originally delivered in 10 second traces. Each seismic line consisted of 51 seismometers called the Z-Land Nodal 3Cs (Fig. 3A) spaced by 20 m for a 1 km line. Along each line were 32 shot locations where 10 shots were executed at each location using the PEG, or Propelled Energy Generator (Fig. 3B).

Fig. 3: Panel A - An image of the Z-Land Nodal 3Cs, which can measure ground displacement in 3 directions. Panel B - An image of the PEG, which launches a metal rod towards a plate on the ground.

Methods

1. Cutting and Resampling Data
Trace length: 10s to 2s
Sampling Frequency: 2000 Hz to 1000 Hz

2. Common Midpoint Gathering
Using source/receiver geometry to group together traces that share common midpoints along ray path

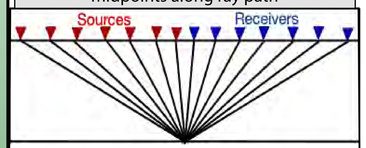

Fig. 4: Illustration of 7 source/receiver pairings all sharing a common midpoint

3. Frequency Filtering
Removing seismic signals whose frequencies lie outside of 70 Hz - 200 Hz

4. Polarization Filtering
Removing seismic signals that are not polarized in the direction of the reflected P-wave polarization

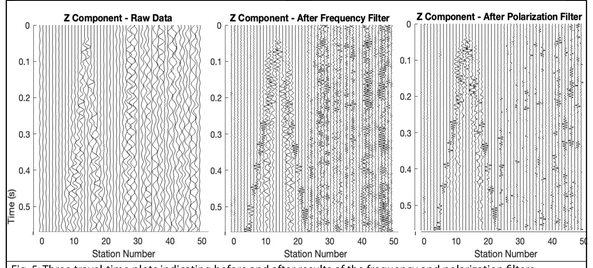

Fig. 5: Three travel-time plots indicating before and after results of the frequency and polarization filters.

5. Normalize
Normalizing each trace by its maximum recorded value to provide a value range of ± 1

6. Phase Muting
Removing waves with well defined seismic velocities (i.e. air wave)

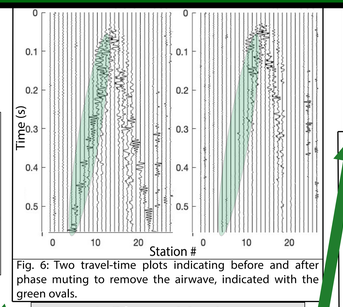

Fig. 6: Two travel-time plots indicating before and after phase muting to remove the airwave, indicated with the green ovals.

7. NMO Correction
Uses velocity sctructure [1] to correct for the normal moveout curve that is a consequence of the CMP gather

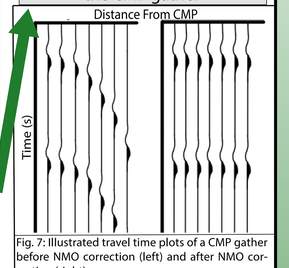

Fig. 7: Illustrated travel time plots of a CMP gather before NMO correction (left) and after NMO correction (right)

Results

- 2-D reflectivity plots do not indicate well defined reflections
- Replot 2-D envelope of reflectivity data
  - Displays wave energy distribution map
- Two sections of low energy occur centered on each line
  - Indicates increased wave attenuation
  - Indicates seismic waves at this location spend more of their ray path in a highly attenuating material than elsewhere

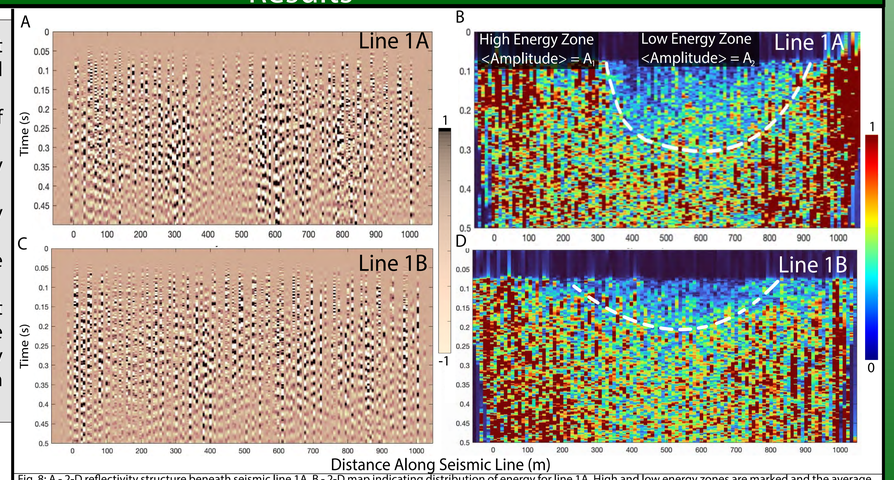

Fig. 8: A - 2-D reflectivity structure beneath seismic line 1A. B - 2-D map indicating distribution of energy for line 1A. High and low energy zones are marked and the average amplitude of these areas were recorded and used for the wave attenuation analysis. C - 2-D reflectivity structure beneath seismic line 1B. D - 2-D map indicating distribution of energy for line 1B. Barrier between high and low energy zones are marked with a white dotted line.

- Reflected seismic waves in column two travel more in highly attenuating material, resulting in less seismic energy reaching receivers above this location
- Column 2 = Low Energy Zone (Fig. 8B)

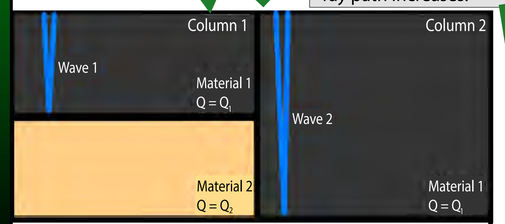

Fig. 9: Hypothetical geological structure. Shown are two columns, the first containing both a highly attenuating material (Material 1 - Basalt) and a low attenuating material (Material 2 - Bedrock). The second column only contains the highly attenuating material.

- For a given quality factor (Q), the measure of a material's ability to pass seismic energy, wave amplitude decreases as its ray path increases.

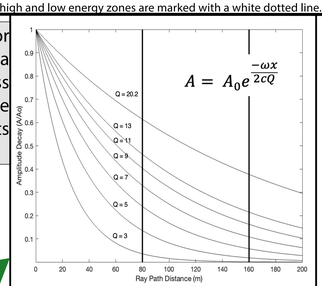

Fig. 10: Plot indicating that seismic wave amplitudes decay more rapidly with lower Q values. Note that ratio of the intersection between the Q curves and two selected distances are plotted in Fig. 12.

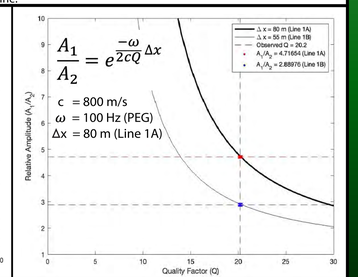

Fig. 11: Plotting the ratio of average amplitudes from lines 1A (red) and 1B (blue), and observing where they intersect the curve given by (1). After obtaining Q from line 1A, the process was reversed with 1B to find the difference in ray path distance Δx.

- Ratio of $\frac{A_1}{A_2}$ (Fig. 7B) allows calculation of quality factor Q (Fig. 9).
  - Q = 20.2
  - Literature shows Q =10-60 for basaltic lava flows [2][3][4]

Conclusions

- Variation in wave amplitudes along the seismic lines indicate there are changes in the amount of wave attenuation being measured
- Larger amounts of attenuation indicate a thickening of the highly attenuating basaltic lava flow
- This thickening is consistent with the additional thickness that would be presesent in a filled grabben structure supporting the hypothesis

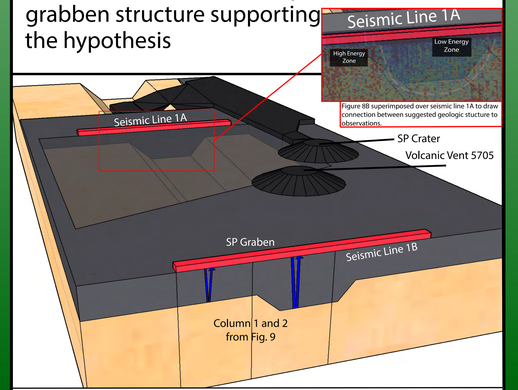

Fig. 12: 3-D rendering of one possible geological structure beneath the SFVF near Vent 5704. A blown up portion of the subsurface below line 1A is displayed with the results in Fig. 7B superimposed on top of it to illustrate the connection between the two. Note the blue arrows benath line 1B, referencing back to Fig. 8 in this poster.

References

[1] Bell, J. E. (2021). Geophysical Exploration of Terrestrial and Lunar Volcanic Fields. [Doctoral Dissertation, University of Maryland – College Park] https://doi.org/10.13016/-po0c-mhot
[2] Clarke, J., Adam, L., van Wijk, K., & Sarout, J. (2020). The influence of fluid type on elastic wave velocity and attenuation in volcanic rocks. Journal of Volcanology and Geothermal Research, 403. https://doi.org/10.1016/j.jvolgeores.2020.107004
[3] Di Martino, M., De Siena, L., Healy, D., & Vialle, S. (2021). Petro-mineralogical controls on coda attenuation in volcanic rock samples. Geophysical Journal International, 226, 1858-1872. https://doi.org/10.1093/gji/ggab198
[4] Maresh, J., White, R. S., Hobbs, R. W., & Smallwood, J. R. (2006). Seismic attenuation of Atlantic margin basalts: Observations and modeling. Geophysics, 71, 211-221. https://-doi.org/10.1190/1.2335875